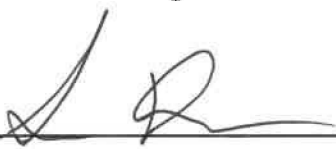# SANDIA NATIONAL LABORATORIES
WASTE ISOLATION PILOT PLANT

ANALYSIS PACKAGE FOR
CUTTINGS, CAVINGS, AND SPALLINGS
IN THE 2019 COMPLIANCE RECERTIFICATION APPLICATION
PERFORMANCE ASSESSMENT (CRA-2019 PA)

REVISION 0

Author:	Dwayne C. Kicker		5/23/2019
	Print	Signature	Date
Technical Reviewer:	Sean Dunagan		5/23/2019
	Print	Signature	Date
QA Reviewer:	Shelly Nielsen		5-23-19
	Print	Signature	Date
Management Reviewer:	R. Chris Camphouse		5-23-19
	Print	Signature	Date

ERMS #571369
MAY 2019
WIPP:4.2.1:PA:QA-L:571155

This page intentionally left blank.

TABLE OF CONTENTS

LIST OF TABLES

LIST OF TABLES (Continued)

LIST OF FIGURES

Executive Summary

The Land Withdrawal Act requires that the U.S. Department of Energy (DOE) apply for recertification of the Waste Isolation Pilot Plant (WIPP) every five years following the initial 1999 waste shipment. The 2019 Compliance Recertification Application (CRA-2019) is the fourth WIPP recertification application submitted for approval by the U.S. Environmental Protection Agency. A performance assessment (PA) has been executed by Sandia National Laboratories in support of the DOE submittal of the CRA-2019. Results found in the CRA-2019 PA are compared to those obtained in the 2014 Compliance Recertification Application (CRA-2014) in order to assess repository performance in terms of the current regulatory baseline. This package documents the direct solids releases analysis component of the CRA-2019 PA. Changes incorporated into the CRA-2019 PA include repository planned changes, parameter updates, and refinements to PA implementation. Changes included in the CRA-2019 PA that potentially affect direct solids releases as compared to the CRA-2014 are:

- Inclusion of an approach to accommodate the operational decisions to not emplace panel closures in Panels 3, 4, 5, and 6.

- Inclusion of an approach to accommodate an additional shaft connecting the repository to the surface, as well as an additional mined region in the repository north end to accommodate drifts that lead to the new shaft.

- Refinement of the gas generation process model to include brine radiolysis.

- Refinement to the corrosion rates of steel under humid and inundated conditions.

- Refinement to the effective shear strength of WIPP waste.

- Updates to WIPP waste inventory parameters.

The primary impacts to direct solids releases from the CRA19 analysis when compared to the CRA14 analysis are as follows:

- Cuttings and cavings area statistics are similar for the CRA19 and CRA14 analyses, with differences attributed to decreasing the lower bound of the TAUFAIL distribution.

- The maximum spallings results for all three replicates of CRA19 and CRA14 are similar for all scenarios. The average spallings release volume for CRA19 is 15% higher compared to CRA14 for the undisturbed scenario (S1-DBR). For scenarios in which the first instrusion passes through a waste-filled panel and into a pressurized brine pocket that may exist under the repository in the Castile formation (scenarios S2-DBR and S3-DBR), the average spallings release volumes for CRA19 are higher (27% to 54% increase) compared to CRA14. For the scenarios that do not pass through a pressurized brine pocket (scenarios S4-DBR and S5-DBR), the average spallings release volumes for CRA19 are slightly lower (5% to 8% decrease) compared to CRA14.

- The cumulative distributions of spallings volumes from all three replicates of both the CRA19 and CRA14 analyses are similar, with larger CRA19 spallings volumes compared to CRA14 at corresponding cumulative frequency levels. The CRA19 analyses result in more simulations with nonzero spallings volumes compared to CRA14.

v

- The overall trend in the CRA19 analysis is toward higher waste region pressures as compared to CRA14, which yields an increase in the spallings volume and in the number of nonzero spallings volumes at all intrusion locations.

- Spallings concentrations (EPA units/m^3) are nearly identical in the CRA19 analysis compared to CRA14 throughout the 10,000-year regulatory period. The similar concentration levels indicate similar levels of EPA units in both the CRA19 and CRA14 analyses.

1.0 INTRODUCTION

The Waste Isolation Pilot Plant (WIPP), located in southeastern New Mexico, has been developed by the U.S. Department of Energy (DOE) for the geologic (deep underground) disposal of transuranic (TRU) waste. Containment of TRU waste at the WIPP is regulated by the U.S. Environmental Protection Agency (EPA) according to the regulations set forth in Title 40 of the Code of Federal Regulations (CFR), Part 191. The DOE demonstrates compliance with the containment requirements according to the Certification Criteria in Title 40 CFR Part 194 by means of performance assessment (PA) calculations performed by Sandia National Laboratories (SNL). WIPP PA calculations estimate the probability and consequence of potential radionuclide releases from the repository to the accessible environment for a regulatory period of 10,000 years after facility closure. The models used in PA are maintained and updated with new information as part of an ongoing process. Improved information regarding important WIPP features, events, and processes typically results in refinements and modifications to PA models and the parameters used in them. Planned changes to the repository and/or the components therein also result in updates to WIPP PA models. WIPP PA models are used to support the repository recertification process that occurs at five-year intervals following the receipt of the first waste shipment at the site in 1999.

PA calculations were included in the 1996 Compliance Certification Application (CCA) (U.S. DOE 1996), and in a subsequent Performance Assessment Verification Test (PAVT) (MacKinnon and Freeze 1997a, 1997b and 1997c). Based in part on the CCA and PAVT PA calculations, the EPA certified that the WIPP met the regulatory containment criteria. The facility was approved for disposal of transuranic waste in May 1998 (U.S. EPA 1998). PA calculations were an integral part of the 2004 Compliance Recertification Application (CRA-2004) (U.S. DOE 2004). During their review of the CRA-2004, the EPA requested an additional PA calculation, referred to as the CRA-2004 Performance Assessment Baseline Calculation (PABC) (Leigh et al. 2005), be conducted with modified assumptions and parameter values (Cotsworth 2005). Following review of the CRA-2004 and the CRA-2004 PABC, the EPA recertified the WIPP in March 2006 (U.S. EPA 2006).

PA calculations were completed for the second WIPP recertification and documented in the 2009 Compliance Recertification Application (CRA-2009). The CRA-2009 PA resulted from continued review of the CRA-2004 PABC, including a number of technical changes and corrections, as well as updates to parameters and improvements to the PA computer codes (Clayton et al. 2008). To incorporate additional information which was received after the CRA-2009 PA was completed, but before the submittal of the CRA-2009, the EPA requested an additional PA calculation, referred to as the 2009 Compliance Recertification Application Performance Assessment Baseline Calculation (PABC-2009) (Clayton et al. 2010), be undertaken which included updated information (Cotsworth 2009). Following the completion and submission of the PABC-2009, the WIPP was recertified in 2010 (U.S. EPA 2010).

PA calculations were completed for the third WIPP recertification and documented in the 2014 Compliance Recertification Application (CRA-2014). Following the completion and submission of the CRA-2014, the WIPP was recertified in 2017 (U.S. EPA 2017).

The Land Withdrawal Act (U.S. Congress 1992) requires that the DOE apply for WIPP recertification every five years following the initial 1999 waste shipment. The 2019 Compliance

Recertification Application (CRA-2019) is the fourth WIPP recertification application submitted by the DOE for EPA approval. The PA executed by SNL in support of the CRA-2019 is detailed in AP-181 (Zeitler 2019a). The CRA-2019 PA includes a repository planned changes, parameter updates, and refinements to PA implementation. Results found in the CRA-2019 PA are compared to those obtained in the CRA-2014 in order to assess repository performance in terms of the current regulatory baseline. This analysis package documents the direct solids releases component of the CRA-2019 PA analysis.

1.1 Changes Since the CRA-2014

Several changes are incorporated in the CRA-2019 PA relative to the CRA-2014 that potentially impact direct solids releases. The changes are:

- Inclusion of an approach to accommodate the operational decisions to not emplace panel closures in Panels 3, 4, 5, and 6.

- Inclusion of an approach to accommodate an additional shaft connecting the repository to the surface, as well as an additional mined region in the repository north end to accommodate drifts that lead to the new shaft.

- Refinement of the gas generation process model to include brine radiolysis.

- Refinement to the corrosion rates of steel under humid and inundated conditions.

- Refinement to the effective shear strength of WIPP waste.

- Updates to WIPP waste inventory parameters.

Changes listed above are discussed in more detail in the sections that follow.

1.2 Overview

Cuttings, cavings, and spallings are the three separate release modes used to determine the quantity of solid waste brought to the surface as the result of a drilling intrusion through a waste panel. Cuttings designates the waste contained in the cylindrical volume created by the cutting action of the drill bit passing through the waste, cavings designates the waste that erodes from the borehole in response to the upward-flowing drilling fluid within the borehole, and spallings designates the waste introduced into the borehole by the release of waste-generated gas escaping to the lower-pressure borehole. The releases associated with these processes are computed within the CUTTINGS_S code.

2.0 CONCEPTUAL APPROACH FOR THE CRA-2019

The PA code CUTTINGS_S calculates the cuttings and cavings areas removed for a set of vectors, scenarios, times, and locations. Cuttings are the solid waste material removed directly by the drill bit intruding into the repository, while cavings are the solid waste material eroded from the walls of the borehole by shear stresses from the circulating drill fluid. CUTTINGS_S also calculates spallings volumes, which are a function of repository pressure. A spallings event is a special case of the drilling intrusion in which the repository contains gas at high pressure that causes (1) localized shear failure of the waste material surrounding the borehole and (2) entrainment of the failed waste material into and up the borehole, carried ultimately to the land surface.

CUTTINGS_S receives inputs from the PA code BRAGFLO, in which BRAGFLO scenarios S1-BF to S5-BF are used to initialize the flow field properties necessary for the calculation of DBRs. This requires that results obtained on the BRAGFLO grid be mapped appropriately to the DBR grid. Code CUTTINGS_S is used to transfer the appropriate scenario results obtained with BRAGFLO to the DBR grid. These transferred flow results are used as initial conditions in the calculation of DBRs. As a result, intrusion scenarios used in the calculation of cuttings, cavings, and spallings correspond to those used in the calculation of DBRs.

2.1 CUTTINGS_S and WIPP PA Intrusion Scenarios

WIPP PA considers five different intrusion scenarios for the calculation of DBRs (Table 1). While CUTTINGS_S uses these standard DBR scenarios as a basis for its calculations, it does so to provide initial conditions for subsequent intrusions in the DBR calculations, rather than modeling the intrusion scenario itself. Thus, in CUTTINGS_S, scenario S1-DBR corresponds to an initial intrusion into the repository, while scenarios S2-DBR through S5-DBR are used to model an intrusion into a repository that has already been penetrated. Two types of intrusions, denoted as E1 and E2, are considered. An E1 intrusion assumes the borehole passes through a waste-filled panel and into a pressurized brine pocket that may exist under the repository in the Castile formation. An E2 intrusion assumes that the borehole passes through the repository but does not encounter a brine pocket. The times at which intrusions are assumed to occur for each scenario are outlined in the last column of Table 1; six intrusion times are modeled for scenario S1-DBR, while five times are modeled for each of scenarios S2-DBR through S5-DBR. Intrusions are assumed to take place in three locations: the southwest waste panel (identified in the CUTTINGS_S output files as location "L"), or in other parts of the repository that are higher in elevation, referred to as North Rest-of-Repository (identified in the CUTTINGS_S output files as location "U") and South Rest-of-Repository (identified in the CUTTINGS_S output files as location "M"). Further details regarding the locations of repository sub-regions are provided by Day (2019).

CUTTINGS_S does not calculate the radioactivity of the material removed; this calculation is performed using CCDFGF, which accounts for stochastic uncertainty in the future of the repository (WIPP PA 2010). The releases associated with cuttings, cavings, and spallings for the CRA-2019 PA can be found in Brunell (2019).

Table 1 – PA intrusion scenarios used in calculating direct solids releases

Scenario	First Intrusion Time and Type year	Intrusion Times – Subsequent year
S1-DBR	None	100, 350, 1000, 3000, 5000, 10000
S2-DBR	350, E1	550, 750, 2000, 4000, 10000
S3-DBR	1000, E1	1200, 1400, 3000, 5000, 10000
S4-DBR	350, E2	550, 750, 2000, 4000, 10000
S5-DBR	1000, E2	1200, 1400, 3000, 5000, 10000

NOTES: For the first intrusions in each scenario, the repository conditions are obtained from BRAGFLO intrusion scenarios. An E1 intrusion scenario is defined as an intrusion into the repository that creates a pathway to a pressurized brine pocket below the repository. An E2 intrusion scenario is defined as an intrusion into the repository that does not create a pathway to a pressurized brine pocket below the repository.

2.2 Cuttings and Cavings

The solid material removed from the repository and carried to the surface by the drilling fluid during the process of drilling a borehole is divided into cuttings and cavings. Cuttings are removed directly by the drill bit, while cavings are eroded from the walls of the borehole by shear stresses from the circulating drill fluid. For the CRA-2019 PA, cuttings and cavings were computed using the same conceptual and numerical models as the CRA-2014; these models are described in the CUTTINGS_S design document (WIPP PA 2004).

CUTTINGS_S calculates the base area of the cylinder of cuttings and cavings removed as a result of a drilling intrusion into the repository. The area of cuttings removed and transported to the surface in the drilling mud corresponds to the drill bit area A_{cut}. The cuttings area A_{cut} and uncompacted volume V_{cut} removed are given by Equations 1 and 2.

$$A_{cut} = \pi D^2 / 4, \tag{1}$$

$$V_{cut} = A_{cut} H = \left(\pi D^2 / 4 \right) H, \tag{2}$$

where $D = 0.31115$ m is the drill bit diameter and $H = 3.96$ m is the uncompacted repository height (WIPP PA 2004). Since the drill bit diameter D and the repository height H are treated as constant parameters, both the drill bit area A_{cut} and cuttings volume V_{cut} are fixed quantities for the CRA-2019 PA.

WIPP PA estimates cavings removal with a model based on the effect of shear stress on the material located adjacent to the edge of the borehole. In particular, material around the edge of the borehole is assumed to shear off until the shear stress on the borehole wall is equal to the shear strength of the waste, which is the maximum shear stress at which erosion of the waste can occur. The process is assumed to be radially symmetric, so that the cavings area is treated as an

annulus formed around the initial cuttings area. For a more detailed discussion of the conceptual model of cavings, see WIPP PA (2004).

2.3 Spallings

Spallings consist of waste that enters the borehole through the release of waste-generated gas escaping into the borehole, which is at a lower pressure than the gas. Calculation of spallings releases for the CRA-2019 PA is divided into four steps (Lord et al. 2003):

1. Characterization of the subjective uncertainty when calculating spallings volumes;

2. Calculation of spallings volumes using DRSPALL to account for subjective uncertainty in waste properties;

3. Interpolation of DRSPALL volumes in CUTTINGS_S to calculate spallings volumes in scenarios for drilling intrusions; and

4. Calculation of spallings releases accounting for stochastic uncertainty in the future of the repository using CCDFGF (WIPP PA 2010).

This section discusses the process used by CUTTINGS_S to calculate spalling volumes for the WIPP drilling intrusion scenarios. For the CRA-2019 PA, an updated version of DRSPALL (version 1.22) is used, which corrects an error found in previous versions (Kicker et al. 2015). Note that in accordance with the planning document (Zeitler 2019a, Section 2), the CRA-2019 PA calculations are compared to CRA-2014 results that have been rerun on the Solaris system with the updated version of DRSPALL (version 1.22).

Additionally, for each vector the code DRSPALL calculates the spallings volume produced for each of four initial repository pressures: $P_1 = 10$ MPa, $P_2 = 12$ MPa, $P_3 = 14$ MPa, and $P_4 = 14.8$ MPa. The lower limit P_1 has been selected as a lower bound as repository pressures below 10 MPa do not yield spallings. Thus, for pressures below P_1, the borehole has a higher pressure than the repository, and therefore the gas will not flow into the borehole (WIPP PA 2004). The upper limit P_4 corresponds to lithostatic pressure; repository pressures above this value lead to repository fracture.

For each vector in a given combination of intrusion scenario, time, and location, the initial repository pressure P is determined using data from previously executed BRAGFLO calculations (Day 2019). If V_i ($i = 1, 2, 3,$ or 4) denotes the volume calculated by DRSPALL corresponding to pressure P_i, CUTTINGS_S calculates the spallings volume V_{spall} as a function of P for a given vector using the formula (WIPP PA 2004) in Equation 3:

$$V_{spall}(P) = \begin{cases} V_1, & \text{for } P \leq P_1 \\ V_i + \dfrac{P-P_i}{P_{i+1}-P_i}(V_{i+1}-V_i), & \text{for } P_i \leq P \leq P_{i+1}, \ i = 1, 2, \text{ or } 3 \\ V_4, & \text{for } P \geq P_4 \end{cases} \tag{3}$$

11

2.4 Direct Brine Release Calculations

Using data from previously executed BRAGFLO calculations, CUTTINGS_S calculates the volume-weighted averages for gas pressure, brine pressure, gas saturation, permeability of rock to brine, and waste room porosity for each user specified zone of the repository. The resulting averages are used as initial conditions for the CRA-2019 PA DBR calculations. For a discussion of the implementation and results of these calculations, see Bethune (2019).

3.0 METHODOLOGY FOR CALCULATING CUTTINGS, CAVINGS, AND SPALLINGS

Analysis plan AP-181 (Zeitler 2019a) explains the methodology used to calculate direct releases (cuttings and cavings, spallings, and DBRs) for the analysis reported here. CUTTINGS_S calculates the quantity of material brought to the surface from a radioactive waste disposal repository as a consequence of an inadvertent human intrusion through drilling, either as cuttings and cavings or as spallings releases and DBRs (WIPP PA 2004). The amount of material removed by cuttings and cavings is reported in terms of the cross-sectional area (m^2), while the amount of material removed by spallings is reported as a volume (m^3), consistent with the output from CUTTINGS_S.

3.1 CUTTINGS_S Calculations

The CRA-2019 PA uses CUTTINGS_S version 6.03. CUTTINGS_S calculates an area for cuttings and cavings and a spallings volume for each combination of replicate, vector, scenario, drilling location, and intrusion time. A total of 23,400 areas (3 replicates × 100 vectors × 3 drilling locations × 26 intrusion times) and 23,400 volumes were determined. A full description of the run control for the CRA19 analysis, including names and locations of input and output files, can be found in Long (2019). As outlined in AP-181 (Zeitler 2019a), in cases where comparisons are made to the CRA-2014 PA results, the CRA14 (Rev. 2) results from the Solaris migration integration tests are used (Kirchner et al. 2014, Kirchner et al. 2015).

3.2 Parameters

The code LHS samples two parameters for CUTTINGS_S calculations (Zeitler 2019b): the effective shear strength for erosion of the waste (BOREHOLE:TAUFAIL) and the drill string angular velocity (BOREHOLE:DOMEGA). The ranges sampled for these variables are shown in Table 2.

In addition to these uncertain parameters, CUTTINGS_S uses a set of constant parameters, listed in Table 3, retrieved from the PA parameter database. Although five of these parameters (BLOWOUT:PARTDIA, all of the DRILLMUD parameters, and WAS_AREA:ABSROUGH) are stored in the PA parameter database as quantities with an associated probability distribution, CUTTINGS_S only uses a single value for each of these parameters. Treating these parameters as constants is a reasonable simplification of the problem based on the results of a sensitivity analysis (Lord et al. 2003). For these parameters, the median value of the distribution is then used as the constant value for CUTTINGS_S. The values in Table 3 have not changed from the CRA-2014 PA, and they apply to the CRA-2019 PA.

Several assumptions were made when determining the CUTTINGS_S parameter values. The major assumptions affecting parameter values are:

- Based upon regulatory guidance in 40 CFR 194 (U.S. EPA 1996), future drilling practices are assumed to be the same as they are at present.

13

Table 2 – Sampled uncertain parameters retrieved from the PA parameter database for cavings calculations

Material	Property	Description	Distribution	Range	Analysis
BOREHOLE	TAUFAIL	Effective shear strength for erosion of the waste	Uniform	2.22 to 77.0 Pa	CRA14
				1.60 to 77.0 Pa	CRA19
BOREHOLE	DOMEGA	Drill string angular velocity	Cumulative	4.2 to 23.0 rad/s	CRA14; CRA19

Table 3 – Constant parameters retrieved from the PA parameter database for cuttings and cavings calculations

Material	Property	Value	Description
BLOWOUT	PARTDIA	2.80000E–03 m	Waste particle diameter [a]
BLOWOUT	HREPO	3.96000E+00 m	Height of repository at burial time
BOREHOLE	DIAMMOD	3.11150E–01 m	Modern or current drill bit diameter
BOREHOLE	COLDIA	2.03200E–01 m	Drill collar diameter
DRILLMUD	DNSFLUID	1.21000E+03 kg/m^3	Density of brine used as drilling fluid (mud) [a]
DRILLMUD	VISCO	9.17000E–03 Pa·s	Viscosity of brine used as drilling fluid (mud) [a]
DRILLMUD	YLDSTRSS	4.40000E+00 Pa	Yield stress point of brine used as drilling fluid (mud) [a]
DRILLMUD	SHEARRT	1020 s^{-1}	Shear rate of the drilling fluid (mud)
DRILLMUD	MUDFLWRT	0.09935 m^3/(m·s)	Drilling fluid (mud) flow rate
WAS_AREA	ABSROUGH	2.50000E–02 m	Absolute roughness of waste material [a]
REFCON	SECYR	3.16888E–08 year/s	Seconds to year conversion
REFCON	PI	3.14159E+00	Reference constant π

[a] This parameter corresponds to a distribution where the "Value" column lists the median value of the distribution, which is treated by CUTTINGS_S as constant.

- The diameter of the intrusion borehole is assumed to be constant at 12.25 inches (0.31115 m). Since the most common bit size used to reach the depth of the repository is 11 inches (U.S. DOE 2018, Figure 2), this assumption can be considered conservative because the volume of cuttings (i.e., the solid waste material removed by the drill bit) increases as the borehole diameter increases. Therefore, a larger borehole diameter results in increased direct solids releases from a borehole intrusion into the repository.

Additional assumptions have also been made about the waste shear strength parameter (BOREHOLE:TAUFAIL); these are discussed in the following section.

3.3 The BOREHOLE:TAUFAIL Parameter

WIPP PA includes scenarios in which human intrusion results in a borehole intersecting the repository. During the intrusion, drilling mud flowing up the borehole will apply a hydrodynamic shear stress on the borehole wall. Erosion of the wall material can occur if this stress is high enough, resulting in a release of radionuclides being carried up the borehole with the drilling mud. The WIPP PA parameter BOREHOLE:TAUFAIL is used to represent the effective shear strength for erosion of WIPP waste.

For the CRA-2014 PA, experimental results from Herrick et al. (2012) were used to determine an updated parameter distribution for BOREHOLE:TAUFAIL (Herrick and Kirchner 2013). Subsequent to the submittal of the CRA-2014, the EPA requested that the DOE reconsider the subset of the Herrick data to be included in the TAUFAIL distribution, including lowering the lower bound of the distribution. The DOE has agreed to its use in the CRA-2019 PA (Zeitler 2019a, Section 2.1.6).

The principal parameters of the probability distribution function for the waste shear strength parameter BOREHOLE:TAUFAIL are shown in Table 4; the cumulative distribution function is plotted in Figure 1.

Table 4 – Principal parameters for the BOREHOLE:TAUFAIL distribution

Attribute	CRA14	CRA19
Distribution type	Uniform	Uniform
Minimum (Pa)	2.22	1.60
Maximum (Pa)	77.00	77.00
Mean (Pa)	39.61	39.30
Median (Pa)	39.61	39.30
Standard deviation (Pa)	21.59	21.766

NOTE: The statistical parameters associated with various distribution types are described by Tierney (1996) with details provided in Appendix A (see worksheet *TAUFAIL*).
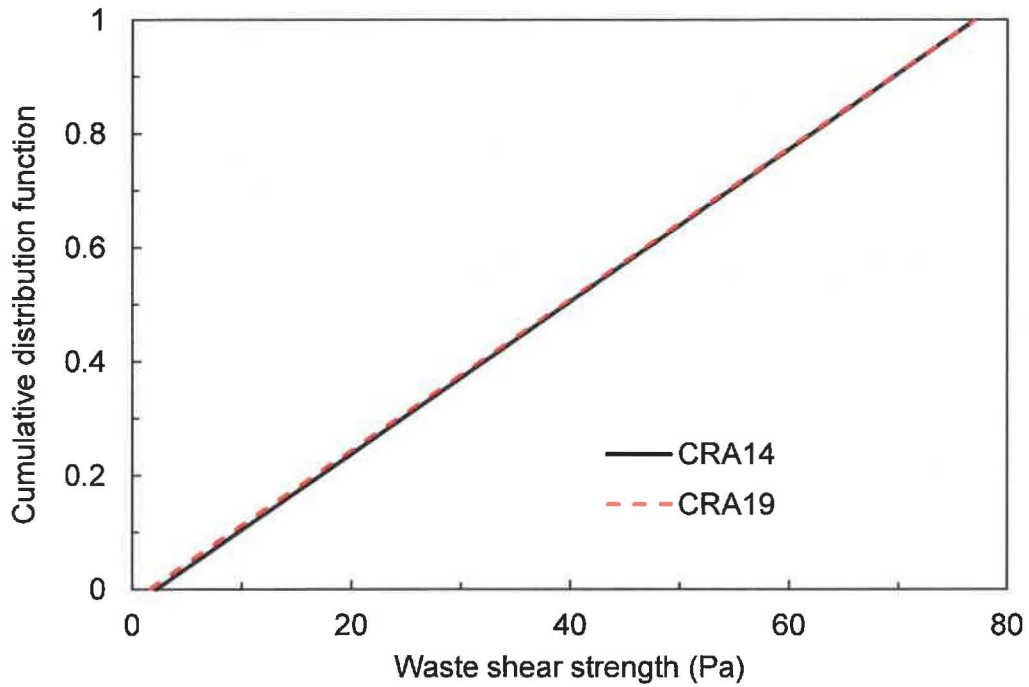
NOTE: Calculation details are provided in Appendix A (see worksheet *TAUFAIL*).

Figure 1 – Cumulative distribution function for the waste shear strength parameter BOREHOLE:TAUFAIL

4.0 RESULTS

The results from CUTTINGS_S are summarized in this section. A Microsoft Excel 2016 spreadsheet was developed to analyze the CUTTINGS_S output and is documented in Appendix A.

4.1 Cuttings and Cavings

Since the drill bit diameter, D (see Borehole Property DIAMMOD in Table 3) is treated as a constant in both the CRA-2014 PA and the CRA-2019 PA, the cuttings area, A_{cut}, is the same for all vectors ($A_{cut} = 0.0760$ m^2, Equation 1).

CUTTINGS_S reports the combined area for cuttings and cavings $A = A_{cut} + A_{cav}$, where A_{cav} is the cavings area. Consequently, the cuttings area A_{cut} must be subtracted from the reported area to determine the cavings area A_{cav} for a given vector. (If $A = A_{cut}$, then no cavings occurs for the given vector.) The results obtained for the CRA-2019 PA are similar to the CRA-2014 PA, with differences attributed to decreasing the lower bound of the TAUFAIL distribution (Section 3.3). The summary of statistics for cavings is shown in Table 5 for both the CRA-2014 and CRA-2019 PAs.

Table 5 – Cavings area statistics for the CRA-2014 and CRA-2019 PAs

| Replicate	Mean Cavings Area (m^2)		Maximum Cavings Area (m^2)		Number of Vectors without Cavings	
	CRA14	CRA19	CRA14	CRA19	CRA14	CRA19
R1	0.010	0.011	0.090	0.110	50	49
R2	0.010	0.010	0.090	0.107	44	44
R3	0.010	0.011	0.075	0.090	50	49

NOTE: Calculation details are provided in Appendix A (see worksheets *cusp_CRA19_r1*, *cusp_CRA19_r2*, *cusp_CRA19_r3*, *CRA14_R1*, *CRA14_R2*, and *CRA14_R3*).

The cumulative frequency of nonzero cavings areas for CRA14 (replicates 1, 2, and 3) and the CRA19 (replicates 1, 2, and 3) is shown in Figure 2. Figure 2 shows that the cumulative distribution of CRA14 is very similar to the cumulative distribution of CRA19. The probability distributions of cavings area from CRA19 and CRA14 analyses are provided in Figure 3, which shows a similar probability frequency of cavings area for both CRA19 and CRA14.
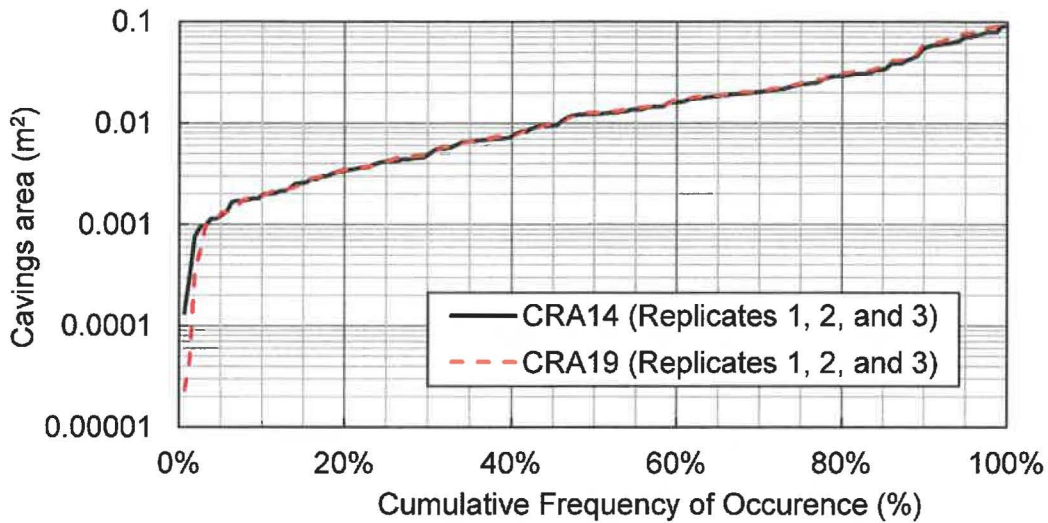
NOTE: Calculation details are provided in Appendix A (see worksheets *Cavings* and *Plots*).

Figure 2 – Cumulative frequency of cavings area
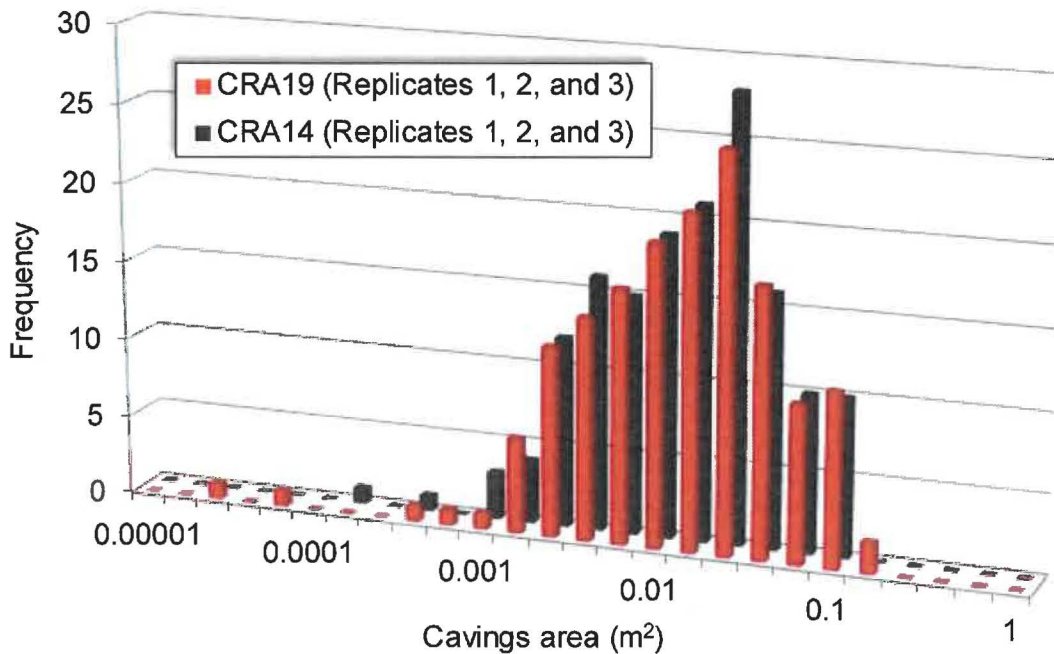
NOTE: Calculation details are provided in Appendix A (see worksheets *Cavings* and *Plots*).

Figure 3 – Probability frequency of cavings area

18

Previous sensitivity analyses have shown that the primary parameters influencing the results of CUTTINGS_S are the waste shear strength and the drill string angular velocity (Vugrin 2005). The cuttings and cavings area for the CRA-2019 PA is plotted against the waste shear strength (Figure 4) and plotted against the drill string angular velocity (Figure 5). While a strong inverse relationship can be seen to exist between waste shear strength and cuttings and cavings area in Figure 4, no correlation between cuttings and cavings area and drill string angular velocity is observed in Figure 5, as nearly identical values of the drill string angular velocity can lead to very different cuttings and cavings areas.
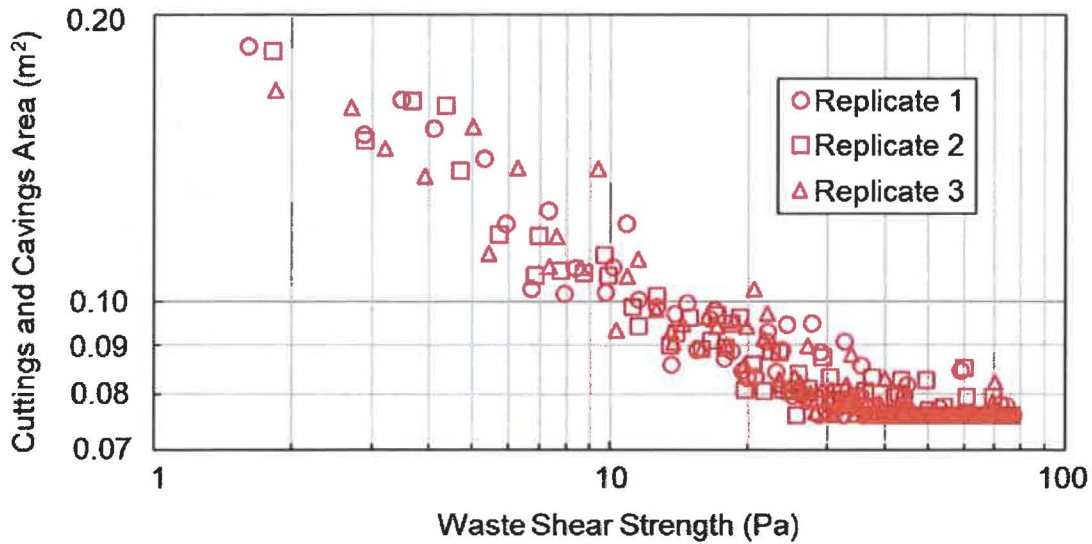
However, plotting cavings areas as a function of both waste shear strength and drill string angular velocity, as in Figure 6, shows that the drill string angular velocity can have a secondary effect on the cavings area, since, for a given waste shear strength, there is a trend towards larger cavings areas as the drill string angular velocity increases.

4.2 Spallings

The cumulative frequency of nonzero spallings volumes for CRA19 and CRA14 (replicates 1, 2, and 3) is shown in Figure 7. This figure provides a summary of all nonzero spallings data from all scenarios, repository regions, and times. Figure 7a considers only those simulations in which spallings occur, showing that the cumulative distributions of spallings volumes from all three replicates of both the CRA19 and CRA14 analyses are similar, with larger CRA19 spallings volumes compared to CRA14 at corresponding cumulative frequency levels. Figure 7b is the same plot except that all spallings results are used, including those simulations where no spallings occur. In this case the CRA19 cumulative distribution of spallings volumes is quite different from the CRA14 results. The shift in the cumulative frequency of occurrence curve for the CRA-2019 spallings volumes (Figure 7b) is the result of more simulations with nonzero spallings.

The change in spallings volumes between the CRA19 and CRA14 is the result of changing repository pressures observed in BRAGFLO calculations for the CRA-2019 PA (Day 2019). The change in pressure within the repository may be attributable to several factors, including (1) the inclusion of an approach to accommodate the operational decisions to not emplace panel closures in Panels 3, 4, 5, and 6, resulting in increased waste contact with brine following an E1 intrusion, (2) the inclusion of an approach to accommodate an additional shaft connecting the repository to the surface, as well as an additional mined region in the repository north end to accommodate drifts that lead to the new shaft, (3) refinement of the gas generation process model to include brine radiolysis, and (4) refinement of the corrosion rate of steel. Because spallings volumes directly depend on repository pressure, an increase in repository pressure translates into larger spallings volumes. Since there is a minimum threshold pressure required to create spallings, an increase in repository pressure also increases the percentage of vectors with spallings.

Spallings concentration (EPA units/m^3) is shown in Figure 8, which depicts near identical concentration in the CRA19 analysis compared to CRA14 throughout the 10,000-year regulatory period. Spalling concentrations are calculated by the PRECCDFGF code as the waste stream volume-averaged concentration of contact-handled waste. The similar concentration levels indicate similar levels of EPA units in both the CRA19 and CRA14 analyses (Kicker 2019).

NOTES: The lower end of the cuttings and cavings area scale, 0.0760 m², corresponds to the limit of zero cavings; the nearly linear trend on the log-log plot indicates a power-law relationship for cuttings and cavings areas as a function of waste shear strength for values of BOREHOLE:TAUFAIL less than about 20 Pa. Calculation details are provided in Appendix A (see worksheets *cusp_CRA19_r1*, *cusp_CRA19_r2*, *cusp_CRA19_r3*, and *Plots*).

Figure 4 – Cuttings and cavings area as a function of waste shear strength for the CRA-2019 PA
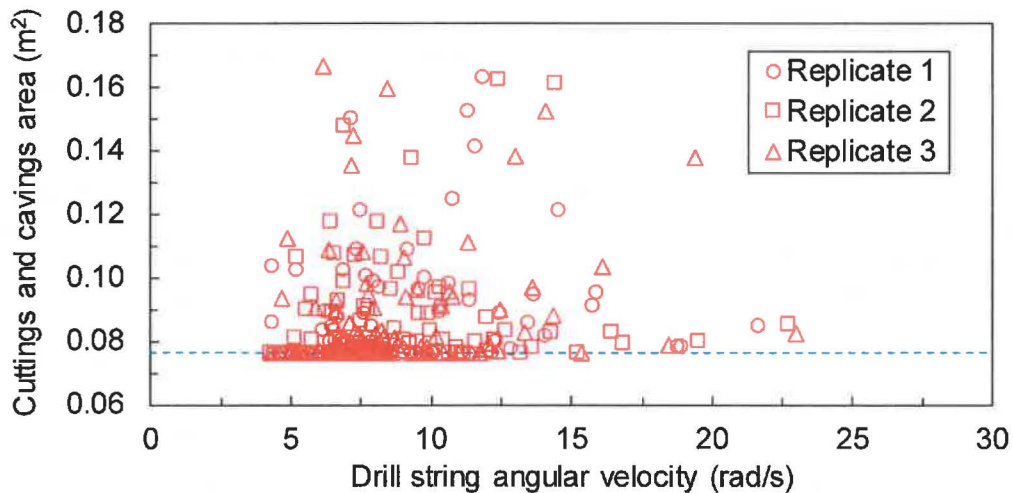
NOTES: The horizontal line indicates the constant cuttings area of 0.0760 m². Calculation details are provided in Appendix A (see worksheets *cusp_CRA19_r1*, *cusp_CRA19_r2*, *cusp_CRA19_r3*, and *Plots*).

Figure 5 – Cuttings and cavings area as a function of drill string angular velocity for the CRA-2019 PA

20
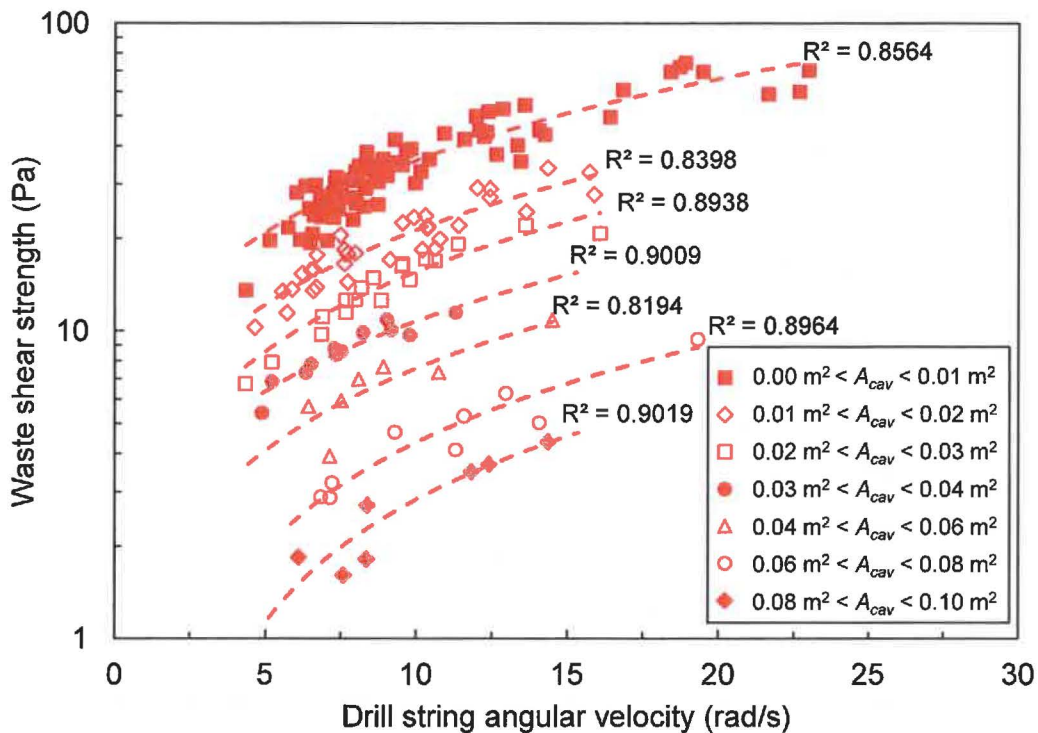
NOTE: Calculation details are provided in Appendix A (see worksheets *R1,R2,R3* and *Plots*).

Figure 6 – Waste shear strength versus drill string angular velocity according to calculated nonzero cavings area for the CRA-2019 PA
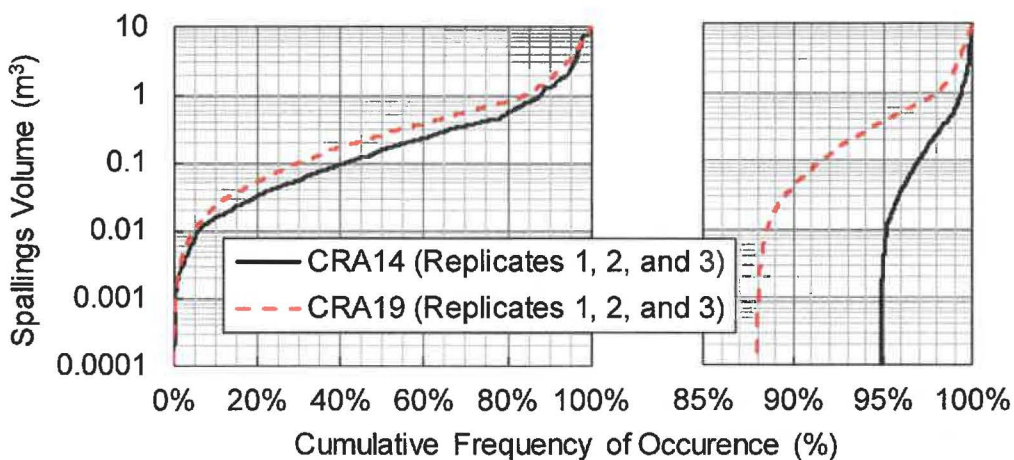
a. Nonzero spallings results — includes only those simulations with spallings

b. All spallings results — includes simulations with no spallings

NOTE: Calculation details are provided in Appendix A (see worksheets *Spallings* and *Plots*).

Figure 7 – Cumulative frequency of spallings volume

NOTE: Calculation details are provided in Appendix A (see worksheets *PRECCDFGF* and *Plots*).

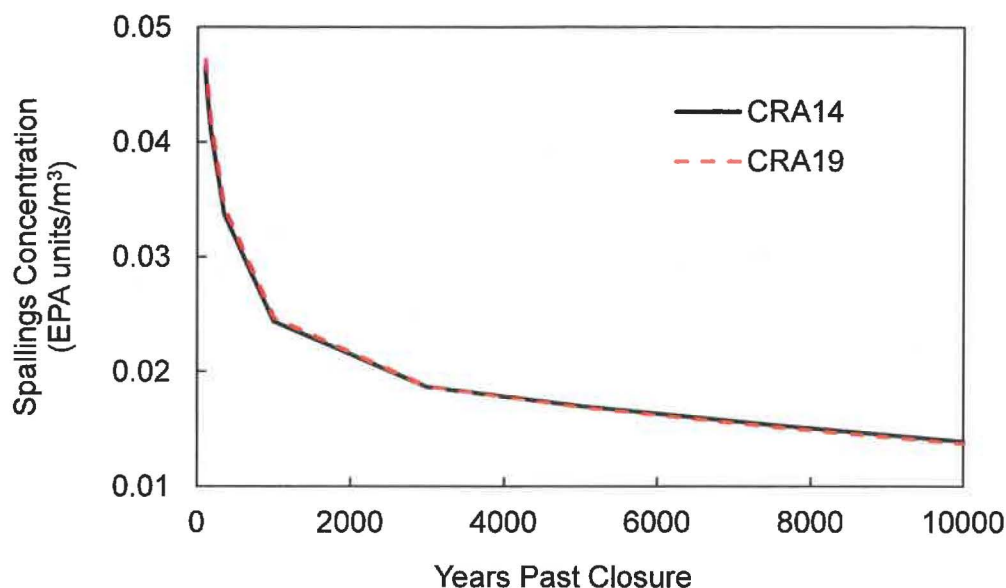## Figure 8 – Spallings concentration from closure to 10,000 years

4.2.1 Spallings Volumes by Scenario

Summary statistics of spallings volumes for the intrusion scenarios considered by CUTTINGS_S are shown in Table 6 for both CRA19 and CRA14 analyses. Results presented in that table are assessed over all three replicates, times, vectors, and drilling locations. The maximum spallings results for all three replicates of CRA19 and CRA14 are similar for all five scenarios. The average spallings release volume for CRA19 is 15% higher compared to CRA14 for the undisturbed scenario (S1-DBR). For scenarios in which the first instrusion passes through a waste-filled panel and into a pressurized brine pocket that may exist under the repository in the Castile formation (scenarios S2-DBR and S3-DBR), the average spallings release volumes for CRA19 are higher (27% to 54% increase) compared to CRA14. For the scenarios that do not pass through a pressurized brine pocket (scenarios S4-DBR and S5-DBR), the average spallings release volumes for CRA19 are slightly lower (5% to 8% decrease) compared to CRA14. However, there is an increase in the number of nonzero spallings in the CRA19 results compared to the CRA14 results across all scenarios. The additional excavation in the repository north end produces a slight reduction in the repository pressure. The operational decisions to not emplace panel closures in Panels 3, 4, 5, and 6 result in greater brine pressures and saturations in the southern half of the repository following Castile intrusions, as the there is no longer a significant barrier to equilibration with the waste panels. Additionally, the refinement of the steel corrosion rate and the refinement of the gas generation process model to include brine radiolysis increase repository pressure in the CRA19 analyses (Day 2019). Consequently, initial intrusions into a previously undisturbed repository result in increases to spallings volumes, as well as increases to the number of nonzero spallings volumes.

22

Table 6 – Summary of spallings releases by scenario

Scenario	Maximum Volume (m³)		Average Nonzero Volume (m³)		Number of Nonzero Volumes (Percentage of Realizations that Result in a Nonzero Spallings Volume)	
	CRA14	CRA19	CRA14	CRA19	CRA14	CRA19
S1-DBR	7.47	7.47	0.63	0.72	200 (3.7%)	258 (4.8%)
S2-DBR	9.84	10.23	0.54	0.83	473 (10.5%)	1254 (27.9%)
S3-DBR	9.80	10.23	0.54	0.68	329 (7.3%)	1063 (23.6%)
S4-DBR	7.47	7.47	0.62	0.59	86 (1.9%)	105 (2.3%)
S5-DBR	7.47	7.47	0.61	0.56	109 (2.4%)	135 (3.0%)

NOTES: Summary results are presented as pooled statistics (combined replicates 1, 2, and 3). Calculation details for CRA19 and CRA14 are provided in Appendix A (see worksheets *cusp_CRA19_r1, cusp_CRA19_r2, cusp_CRA19_r3, CRA14_R1, CRA14_R2,* and *CRA14_R3*).

4.2.2 Spallings Volumes by Location

Examining spallings releases as a function of intrusion location in Table 7 shows that for CRA19 analyses, releases are largest for intrusions into the waste panel (Lower Region) and into the South Rest-of-Repository (Middle Region). Intrusions into the North Rest-of-Repository (Upper Region) area leads to releases that are smaller in magnitude. The spallings releases for CRA19 results are larger in magnitude across all three intrusion locations compared to CRA14. The maximum volumes and the number of nonzero volumes in all regions and all replicates of CRA19 are higher compared to CRA14. The average nonzero volumes in the Lower and Middle regions of CRA19 are higher (10% to 54% increase) compared to CRA14, while the average volume in the Upper Region is slightly lower (4% decrease) for CRA19.

The additional excavation in the repository north end produces a reduction in the repository pressure. The decrease in waste panel pressure translates to decreases in spallings volumes and the number of nonzero spallings volumes in the North Rest-of-Repository (Upper Region) compared to the Lower and Middle Regions for the CRA-2019 PA. The operational decisions to not emplace panel closures in Panels 3, 4, 5, and 6 result in increased communication between the waste panel and South Rest-of-Repository areas and allows for greater brine pressures and saturations in the South Rest-of-Repository area following Castile intrusions, as the there is no longer a significant barrier to equilibration with the waste panel. Additionally, the refinement of the steel corrosion rate and the refinement of the gas generation process model to include brine radiolysis increase repository pressure in the CRA19 analyses. Further details regarding the locations of repository sub-regions and repository pressures are provided by Day (2019).

Table 7 – Summary of spallings as a function of intrusion location

Intrusion Location	Maximum Volume (m³)		Average Nonzero Volume (m³)		Number of Nonzero Volumes (Percentage of Realizations that Result in a Nonzero Spallings Volume)	
	CRA14	CRA19	CRA14	CRA19	CRA14	CRA19
Lower Region (Waste Panel)	9.84	10.23	0.49	0.76	770 (9.9%)	1135 (14.6%)
Middle Region (South Rest-of-Repository)	7.47	10.23	0.68	0.75	240 (3.1%)	1128 (14.5%)
Upper Region (North Rest-of-Repository)	7.47	9.85	0.73	0.71	187 (2.4%)	552 (7.1%)

NOTES: Summary results are presented as pooled statistics (combined replicates 1, 2, and 3). Calculation details for CRA19 and CRA14 are provided in Appendix A (see worksheets *cusp_CRA19_r1a*, *cusp_CRA19_r2a*, *cusp_CRA19_r3a*, *CRA14_R1a*, *CRA14_R2a*, and *CRA14_R3a*).

5.0 SUMMARY

The primary impacts to direct solids releases from the CRA19 analysis when compared to the CRA14 analysis are as follows:

- Cuttings and cavings area statistics are similar for the CRA19 and CRA14 analyses, with differences attributed to decreasing the lower bound of the TAUFAIL distribution (see Section 3.3)

- The maximum spallings results for all three replicates of CRA19 and CRA14 are similar for all scenarios. The average spallings release volume for CRA19 is 15% higher compared to CRA14 for the undisturbed scenario (S1-DBR). For scenarios in which the first instrusion passes through a waste-filled panel and into a pressurized brine pocket that may exist under the repository in the Castile formation (scenarios S2-DBR and S3-DBR), the average spallings release volumes for CRA19 are higher (27% to 54% increase) compared to CRA14. For the scenarios that do not pass through a pressurized brine pocket (scenarios S4-DBR and S5-DBR), the average spallings release volumes for CRA19 are slightly lower (5% to 8% decrease) compared to CRA14.

- The additional excavation in the repository north end produces a reduction in the repository pressure. The decrease in waste panel pressure translates to decreases in spallings volumes and the number of nonzero spallings volumes in the North Rest-of-Repository (Upper Region) compared to the Lower and Middle Regions for the CRA-2019 PA.

- The operational decisions to not emplace panel closures in Panels 3, 4, 5, and 6 result in increased communication between the waste panel and South Rest-of-Repository areas and allows for greater brine pressures and saturations in the South Rest-of-Repository area following Castile intrusions, as the there is no longer a significant barrier to equilibration with the waste panel. Additionally, the refinement of the steel corrosion rate and the refinement of the gas generation process model to include brine radiolysis increase repository pressure in the CRA19 analyses.

- The cumulative distributions of spallings volumes from all three replicates of both the CRA19 and CRA14 analyses are similar, with larger CRA19 spallings volumes compared to CRA14 at corresponding cumulative frequency levels. The CRA19 analyses result in more simulations with nonzero spallings volumes compared to CRA14.

- The overall trend in the CRA19 analysis is toward higher waste region pressures as compared to CRA14, which yields an increase in the spallings volume and in the number of nonzero spallings volumes at all intrusion locations.

- Spallings concentrations (EPA units/m^3) are nearly identical in the CRA19 analysis compared to CRA14 throughout the 10,000-year regulatory period. The similar concentration levels indicate similar levels of EPA units in both the CRA19 and CRA14 analyses.

This page intentionally left blank.

6.0 REFERENCES

Bethune, J. 2019. *Analysis Package for Direct Brine Releases in the 2019 Compliance Recertification Application Performance Assessment (CRA-2019 PA)*. Sandia National Laboratories, Carlsbad, NM. ERMS 571370.

Brunell, S. 2019. *Analysis Package for Normalizied Releases in the 2019 Compliance Recertification Application Performance Assessment (CRA-2019)*. Sandia National Laboratories, Carlsbad, NM. ERMS 571373.

Clayton, D.J., S. Dunagan, J.W. Garner, A.E. Ismail, T.B. Kirchner, G.R. Kirkes, M.B. Nemer 2008. *Summary Report of the 2009 Compliance Recertification Application Performance Assessment*. Sandia National Laboratories, Carlsbad, NM. ERMS 548862.

Clayton, D.J., R.C. Camphouse, J.W. Garner, A.E. Ismail, T.B. Kirchner, K.L. Kuhlman, and M.B. Nemer 2010. *Summary Report of the CRA-2009 Performance Assessment Baseline Calculation*. Sandia National Laboratories, Carlsbad, NM. ERMS 553039.

Cotsworth, E. 2005. *EPA Letter on Conducting the Performance Assessment Baseline Change (PABC) Verification Test*. U.S. EPA, Office of Radiation and Indoor Air, Washington, D.C. ERMS 538858.

Cotsworth, E. 2009. *EPA Letter on CRA-2009 First Set of Completeness Comments*. U.S. EPA, Office of Radiation and Indoor Air, Washington, D.C. ERMS 551444.

Day, B. 2019. *Analysis Package for Salado Flow in the 2019 Compliance Recertification Application Performance Assessment (CRA-2019 PA)*. Sandia National Laboratories, Carlsbad, NM. ERMS 571368.

Herrick, C.G., M.D. Schuhen, D.M. Chapin, and D.C. Kicker 2012. *Determining the Hydrodynamic Shear Strength of Surrogate Degraded TRU Waste Materials as an Estimate for the Lower Limit of the Performance Assessment Parameter TAUFAIL*. Revision 0. Sandia National Laboratories, Carlsbad, NM. ERMS 558479.

Herrick, C.G. and T. Kirchner 2013. *Follow-up to Questions Concerning TAUFAIL Flume Testing Raised During the November 14-15, 2012 Technical Exchange Between the DOE and EPA*. Memo to C. Camphouse, January 24, 2013. Sandia National Laboratories, Carlsbad, NM. ERMS 559081.

Kicker, D.C. 2019. *Analysis Package for Inventory EPA Units in the 2019 Compliance Recertification Application Performance Assessment (CRA-2019 PA)*, Revision 0. Carlsbad, New Mexico: Sandia National Laboratories. ERMS 571372.

Kicker, D.C., C. Herrick, and T. Zeitler. 2015. *Impact of the DRSPALL Modification on Waste Isolation Pilot Plant Performance Assessment Calculations*. Sandia National Laboratories, Carlsbad, NM. ERMS 564863.

Kirchner, T., A. Gilkey, and J. Long. 2014. *Summary Report on the Migration of the WIPP PA Codes from VMS to Solaris*, AP-162 Revision 1. Sandia National Laboratories, Carlsbad, NM. ERMS 561757.

Kirchner, T., A. Gilkey, and J. Long. 2015. *Addendum to the Summary Report on the Migration of the WIPP PA Codes from VMS to Solaris*, AP-162. Sandia National Laboratories, Carlsbad, NM. ERMS 564675.

Leigh, C.D., J.F. Kanney, L.H. Brush, J.W. Garner, G.R. Kirkes, T. Lowry, M.B. Nemer, J.S. Stein, E.D. Vugrin, S. Wagner, and T.B. Kirchner 2005. *2004 Compliance Recertification Application Performance Assessment Baseline Calculation*, Revision 0. Sandia National Laboratories, Carlsbad, NM. ERMS 541521.

Long, J.J. 2019. *Computational Code Execution and File Management for the 2019 Compliance Recertification Application Performance Assessment (CRA-2019 PA)*. Sandia National Laboratories, Carlsbad, NM. ERMS 571375.

Lord, D., D. Rudeen, and C. Hansen 2003. *Analysis Package for DRSPALL: Compliance Recertification Application: Part I—Calculation of Spall Volumes*. Sandia National Laboratories, Carlsbad, NM. ERMS 532766.

MacKinnon, R.J. and G. Freeze 1997a. *Summary of EPA-Mandated Performance Assessment Verification Test (Replicate 1) and Comparison With the Compliance Certification Application Calculations*. Revision 1. Sandia National Laboratories, Carlsbad, NM. ERMS 422595.

MacKinnon, R.J. and G. Freeze 1997b. *Summary of Uncertainty and Sensitivity Analysis Results for the EPA-Mandated Performance Assessment Verification Test*. Revision 1. Sandia National Laboratories, Carlsbad, NM. ERMS 420669.

MacKinnon, R.J. and G. Freeze 1997c. *Supplemental Summary of EPA-Mandated Performance Assessment Verification Test (All Replicates) and Comparison With the Compliance Certification Application Calculations*. Revision 1. Sandia National Laboratories, Carlsbad, NM. ERMS 414880.

Tierney, M.S. 1996. *Distributions*. Memo to Distribution, March 21, 1996. Sandia National Laboratories, Carlsbad, NM. ERMS 235268.

U.S. Congress 1992. *WIPP Land Withdrawal Act*. Public Law 102-579, 106 Stat. 4777, 1992; as amended by Public Law 104-201, 110 Stat. 2422, 1996.

U.S. Department of Energy (DOE) 1996. *Title 40 CFR Part 191 Compliance Certification Application for the Waste Isolation Pilot Plant*. DOE/CAO-1996-2184. U.S. Department of Energy, Waste Isolation Pilot Plant, Carlsbad Area Office. Carlsbad, NM.

U.S. DOE 2004. *Title 40 CFR Part 191 Subparts B and C Compliance Recertification Application for the Waste Isolation Pilot Plant*. DOE/WIPP 2004-3231. U.S. Department of Energy, Carlsbad Area Office, Carlsbad, NM.

U.S. DOE 2018. *Delaware Basin Monitoring Annual Report*. DOE/WIPP-18-2308 Rev. 1. U.S. Department of Energy, Carlsbad Area Office, Carlsbad, NM.

U.S. Environmental Protection Agency (EPA) 1996. *40 CFR 194, Criteria for the Certification and Recertification of the Waste Isolation Pilot Plant's Compliance with the 40 CFR Part 191 Disposal Regulations*. Washington, DC: United States Environmental Protection Agency.

U.S. EPA 1998. *40 CFR 194, Criteria for the Certification and Recertification of the Waste Isolation Pilot Plant's Compliance with the Disposal Regulations: Certification Decision: Final Rule*. Federal Register. ERMS 251924.

U.S. EPA 2006. *40 CFR 194, Criteria for the Certification and Recertification of the Waste Isolation Pilot Plant's Compliance with the Disposal Regulations: Certification Decision: Final Rule*. Federal Register, Vol. 71, 18010-18021.

U.S. EPA 2010. *40 CFR 194, Criteria for the Certification and Recertification of the Waste Isolation Pilot Plant's Compliance with the Disposal Regulations: Recertification Decision*. Federal Register No. 222, Vol. 75, pp. 70584-70595, November 18, 2010.

U.S. EPA 2017. *Criteria for the Certification and Recertification of the Waste Isolation Pilot Plant's Compliance with the Disposal Regulations; Recertification Decision*. July 19, 2017. Office of Radiation and Indoor Air, Docket EPA-HQ-OAR-2014-0609-0079.

Vugrin, E.D. 2005. *Analysis Package for CUTTINGS_S, CRA 2004 Performance Assessment Baseline Calculation*. Sandia National Laboratories, Carlsbad, NM. ERMS 540468.

WIPP PA 2004. *Design Document for CUTTINGS_S Version 6.00*. Sandia National Laboratories, Carlsbad, NM. ERMS 537038.

WIPP PA 2010. *Design Document and User's Manual for CCDFGF Version 7.00*. Sandia National Laboratories, Carlsbad, NM. ERMS 554046.

Zeitler, T.R. 2019a. *Analysis Plan for the 2019 WIPP Compliance Recertification Application Performance Assessment*. AP-181. Revision 0. Sandia National Laboratories, Carlsbad, NM. ERMS 571150

Zeitler, T.R. 2019b. *Analysis Package for Parameter Sampling in the 2019 Compliance Recertification Application Performance Assessment (CRA-2019 PA)*. Sandia National Laboratories, Carlsbad, NM. ERMS 571367.

This page intentionally left blank.

APPENDIX A — EXCEL FILE FOR ANALYZING CUTTINGS_S RESULTS

This appendix provides information on the Microsoft Excel® 2016 file used to analyze the results obtained from CUTTINGS_S as part of the CRA-2019 PA calculations. The Excel file, *cusp_CRA19_R0.xlsx*, was developed on a PC workstation running Windows 10 Enterprise and is included as a machine readable (DVD) supplement to this analysis package.

A.1 Inputs

Inputs for the Excel file, *cusp_CRA19_R0.xlsx*, include CUTTINGS_S output files (located on the Sun Solaris cluster at /nfs/data/CVSLIB/WIPP_ANALYSES/CRA19/CUTTINGS_S/ Output):

- *cusp_CRA19_r1.tbl*
- *cusp_CRA19_r2.tbl*
- *cusp_CRA19_r3.tbl.*

Additional inputs are provided by LHS output files (located on the Sun Solaris cluster at /nfs/data/CVSLIB/WIPP_ANALYSES/CRA19/LHS/Output):

- *lhs2_CRA19_r1_con.trn*
- *lhs2_CRA19_r2_con.trn*
- *lhs2_CRA19_r3_con.trn.*

and PRECCDFGF output file, *ccgf_CRA19_reltab_r1.dat* (located on the Sun Solaris cluster at /nfs/data/CVSLIB/WIPP_ANALYSES/CRA19/PRECCDFGF/Output).

CUTTINGS_S output files for CRA14 (*cusp_CRA14_r1.tbl*, *cusp_CRA14_r2.tbl*, and *cusp_CRA14_r3.tbl*) were used as inputs to *cusp_CRA19_R0.xlsx* to develop CRA14 data summaries to compare to CRA19 results. These input files are located on the Sun Solaris cluster at /nfs/data/CVSLIB/WIPP_ANALYSES/CRA14/CUTTINGS_S/Output. Also, PRECCDFGF output file for CRA14, *ccgf_CRA14_reltab_r1.dat* (located on the Sun Solaris cluster at /nfs/ data/CVSLIB/WIPP_ANALYSES/CRA14/PRECCDFGF/Output) was used to compare to CRA19 results.

A.2 Description

The calculations in the file process and summarize the output from CUTTINGS_S, including the tabulated results shown in Tables 4 through 7 and the graphical output shown in Figures 1 through 8. Excel file *cusp_CRA19_R0.xlsx* contains multiple worksheets described as follows:

- **cusp_CRA19_r1.** This worksheet calculates summary statistics for CRA19 Replicate 1 obtained from CUTTINGS_S output file *cusp_CRA19_r1.tbl*, including spallings volumes by scenario.
- **cusp_CRA19_r1a.** This worksheet calculates summary statistics for CRA19 Replicate 1 obtained from CUTTINGS_S output file *cusp_CRA19_r1.tbl*, including spallings volumes by location.

- **cusp_CRA19_r2.** This worksheet calculates summary statistics for CRA19 Replicate 2 obtained from CUTTINGS_S output file *cusp_CRA19_r2.tbl*, including spallings volumes by scenario.
- **cusp_CRA19_r2a.** This worksheet calculates summary statistics for CRA19 Replicate 2 obtained from CUTTINGS_S output file *cusp_CRA19_r2.tbl*, including spallings volumes by location.
- **cusp_CRA19_r3.** This worksheet calculates summary statistics for CRA19 Replicate 3 obtained from CUTTINGS_S output file *cusp_CRA19_r3.tbl*, including spallings volumes by scenario.
- **cusp_CRA19_r3a.** This worksheet calculates summary statistics for CRA19 Replicate 3 obtained from CUTTINGS_S output file *cusp_CRA19_r3.tbl*, including spallings volumes by location.
- **R1,R2,R3.** This worksheet provides pooled summary output data for CRA19 Replicates 1, 2, and 3, including drill string angular velocity (parameter BOREHOLE:DOMEGA), waste shear strength (parameter BOREHOLE:TAUFAIL), and CUTTINGS_S output data sorted by cavings area, A_{cav}. Note that in each replicate, every set of 100 vectors contain identical A_{cav} values. Therefore, only the first set of 100 vectors from each output file are included.
- **TAUFAIL.** This worksheet calculates parameters for BOREHOLE:TAUFAIL, which is the waste shear strength (Pa). The distribution type, minimum and maximum values are stored in the WIPP PA parameter database. The Expected Value (Pa), Variance (Pa^2), Standard Deviation (Pa), Median (Pa), and Distribution Function are calculated based on the calculation approach provided by Tierney (1996).
- **Cavings.** This worksheet calculates the cumulative frequency of cavings area (A_{cav}) for both CRA19 and CRA14. Only the first set of 100 vectors in each replicate is included this data, because each set of 100 vectors contain identical A_{cav} values. All rows containing no cavings area (note that any value of A_{cav} less than 0.0000001 is considered to be zero) were deleted so that only nonzero cavings areas are included.
- **Spallings.** This worksheet calculates the cumulative frequency of spallings volume for both CRA19 and CRA14.
- **PRECCDFGF.** This worksheet presents spallings concentration for Replicate 1 from closure to 10,000 years for both CRA19 and CRA14.
- **Plots.** This worksheet generates the following plots:
    - Figure 1. This chart plots waste shear strength data from worksheet *TAUFAIL*.
    - Figure 2. This chart plots cumulative frequency of cavings area data from worksheet *Cavings*.
    - Figure 3. This chart plots probability frequency of cavings area data from worksheet *Cavings*.
    - Figure 4. This chart plots cuttings and cavings area data versus waste shear strength from worksheets *cusp_CRA19_r1*, *cusp_CRA19_r2*, and *cusp_CRA19_r3*.
    - Figure 5. This chart plots cuttings and cavings area data versus drill string angular velocity from worksheets *cusp_CRA19_r1*, *cusp_CRA19_r2*, and *cusp_CRA19_r3*.
    - Figure 6. This chart plots waste shear strength data versus drill string angular velocity from worksheet *R1,R2,R3*.

- Figure 7. This chart plots cumulative frequency of spallings volume data from worksheet *Spallings*.
- Figure 8. This chart plots spallings concentration data versus years past closure from worksheet *PRECCDFGF*.

- **CRA14_R1.** This worksheet calculates summary statistics for CRA14 Replicate 1 obtained from CUTTINGS_S output file *cusp_CRA14_r1.tbl*, including spallings volumes by scenario.
- **CRA14_R1a.** This worksheet calculates summary statistics for CRA14 Replicate 1 obtained from CUTTINGS_S output file *cusp_CRA14_r1.tbl*, including spallings volumes by location.
- **CRA14_R2.** This worksheet calculates summary statistics for CRA14 Replicate 2 obtained from CUTTINGS_S output file *cusp_CRA14_r2.tbl*, including spallings volumes by scenario.
- **CRA14_R2a.** This worksheet calculates summary statistics for CRA14 Replicate 2 obtained from CUTTINGS_S output file *cusp_CRA14_r2.tbl*, including spallings volumes by location.
- **CRA14_R3.** This worksheet calculates summary statistics for CRA14 Replicate 3 obtained from CUTTINGS_S output file *cusp_CRA14_r3.tbl*, including spallings volumes by scenario.
- **CRA14_R3a.** This worksheet calculates summary statistics for CRA14 Replicate 3 obtained from CUTTINGS_S output file *cusp_CRA14_r3.tbl*, including spallings volumes by location.

This page intentionally left blank.